CHAPTER 138

Velocity Field Measurements over Breakwater Heads under 3D Waves

Yoshiharu Matsumi [1], Akira Kimura [2] and Kenichi Ohno [3]

Abstract

The measurements of wave kinematics over the breakwater heads under uni and multidirectional waves attack were undertaken to achieve an improved understanding of the influence of wave directionality on the stability of heads. The characteristics of the magnitudes and directions of velocity vectors under 3D waves were assessed by comparing with those measured under 2D waves. The sensitive zones of the initial damage in the head sections were evaluated by linking the measurements of velocity components with a stability formula for armour stones on the heads, which was derived in this study.

Introduction

Breakwater designs have been generally evaluated using unidirectional waves, because they are widely considered to be conservative. This may be true for the trunk section of the breakwater where the directional spread associated with the multidirectional seas tends to reduce the wave loads imparted on the structure. However, for the breakwater heads, multidirectional waves could be expected to induce more loads on the structure due to their geometry.

The previous study which was carried out by Matsumi and Mansard et al. (1994), was the first step towards an experimental program achieving the realistic stability criteria for breakwater heads under multidirectional seas. It presented a comparison for the performance of breakwater heads under 2D and 3D waves attack. However, those experimental results could not draw general conclusion that the head sections were prone to more or less damage under 3D waves.

---

1   Associate Professor, D. Eng., Dept. of Social Systems Eng., Tottori University, Tottori 680, Japan.
2   M. ASCE, Professor, D. Eng., Dept. of Social Systems Eng., Tottori University
3   Graduate Student, M. Eng., Dept. of Social Systems Eng., Tottori University

The objective of this study is, as a continuation of that program, to explore a better insight into the reasons for the damage results of the heads in previous study through the measurements of wave kinematics over the heads under uni and multidirectional waves. Furthermore, directly unexpected waves attack under 3D waves may lead to higher loads to armour stones at some local position in the heads. Namely, the locality in location of the sensitive zones of the initial damage in the heads for 3D waves is deemed to be stronger than the case of 2D waves. This initiation of damage is relevant to trigger of breakwater failure. Therefore, the second purpose is to investigate the locality in spatial occurrence of the initial damage over the heads for 2D and 3D waves, which is evaluated by linking the measurements of velocity components with a stability formula for the armour stone.

Experimental Setup

Layout of the basin

The physical model tests were carried out, at the Tottori university, in the multidirectional wave basin with a length of 14m and a wide of 8.4m. Figure 1 shows a plan view of the experimental set-up. A fourteen-segment generator of the snake type is located along one of the 8.4m sides of the basin. Expanded polystyrene absorbers with permeability, capable of limiting wave reflections to 20% for most frequencies of interest, are installed along the two sides of the basin. On the side opposite the wave generator, the slope with 1:10 is placed in order to ensure an efficient dissipation of wave energy.

Layout of current meters and wave gauges

The velocity field over the head was measured using 6 bi-axial electromagnetic current meters at 6 different locations indicated by dotes in Figure 1. The positions of these probes were fixed before placing the structure. The initial deflection of the U and V components of each current meter, by placing against the coordinate system located in the basin, was established by means of the preliminary regular wave tests without the breakwater. In Figure 1, θ shows the directions of velocity vector, minus θ and V(-) velocity component indicate flow towards armour layer of the head. The water surface elevations of the sea states in the proximity of the model were measured using 8 wave gauges at 8 different locations.

Layout of breakwater model

The layout of the breakwater model had to be designed carefully to ensure homogeneous sea states on the breakwater. For this purpose, the numerical model which was based on the diffraction theory and boundary integral equation was used. This model, developed by Isaacson (1992), can predict the water surface elevation and kinematics of the sea states prevailing at different locations in the basin. A

sample output resulting from this numerical model is presented in Figure 2. It illustrates the spatial distribution of wave heights in the basin without the breakwater model in place, under a multidirectional sea state. The expected wave heights presented in this figure were normalized with respect to target wave height. Note that their maximum value is only 0.9. This is due to the diffraction processes and can be increased by applying an amplification factor. It can be seen from this figure that the useful test area, over which the sea state is homogeneous, is limited by a triangular boundary. According to this figure, the best location for the model would be close to the paddle. However, since this wave basin is not yet equipped with active absorption, in order to minimize re-reflections from the paddles, the model is placed with its longitudinal axis rotated 20° with respect to the paddles, as shown in Figure 1.
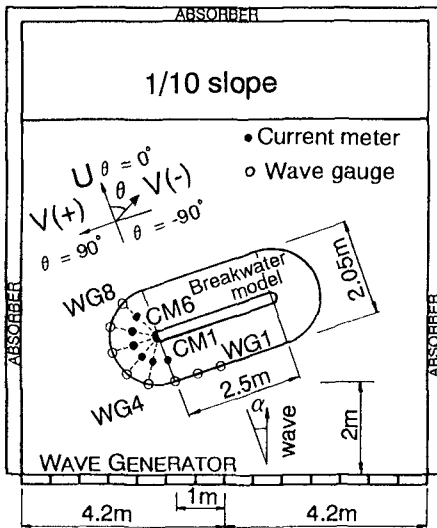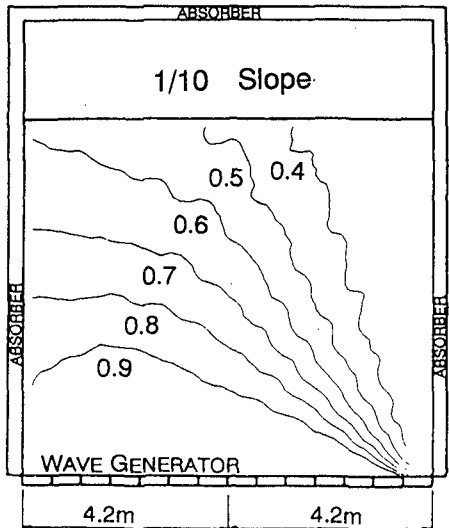

Figure 1 Plan view of the experimental set-up.

Figure 2 Spatial distribution of wave heights in the basin without the model.

Characteristics of the breakwater model

Figure 3 shows both plan and profile views of the breakwater model. The three dimensional rubble-mound breakwater with 2 layers of armour stones and a relatively porous core was built with a slope of 1:2. Its height was 50cm and it performed as a non-overtopping structure in a water depth of 30cm. Since this study was to focus on the wave velocity field over the heads without any damage, the whole surface of breakwater was covered with a hard nylon mesh to restrain armor stones. The reflection characteristics of the breakwater were estimated under unidirectional waves of normal incidence. The reflection coefficient was about 25%.

The characteristics of the armour and core stones used in the experiments are presented in Table 1. The weight of armour stones, W_{50}, was 42 grams, this value was 1.5 times the weight estimated by van der Meer's formula (1987) with damage parameter S=2 against the targeted significant wave height, H_{m0}=6cm, and peak wave period, Tp=1.4s. The gradations of armour stones were meticulously checked and the resulting D_{n85}/D_{n15} ratio for the armour was 1.1.
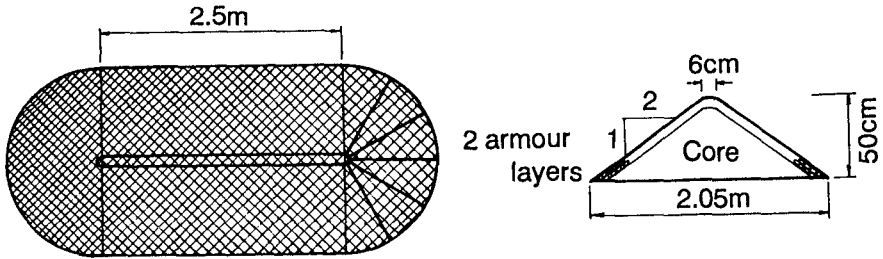

Figure 3 Plan and profile view of the breakwater model.

Table 1 Summary of the breakwater characteristics.

W_{50} weight of armour (g)	42
W_{a50} weight of core (g)	3.75
D_{n50} weight of armour (cm)	2.51
Porosity	0.45
D_L Length of head (cm)	205
T_L Length of trunk (cm)	250
Crest breadth (cm)	6
Height of breakwater (cm)	50

$$D_{n50} = \left(W_{50} / \rho_s \right)^{1/3} \quad , \rho_s : \text{unit weight of armour stone}$$

Table 2 Characteristics of waves in experiments.

Spectrum	Tp (s)	γ	H_{m0} (cm)	α (deg.)	S_{max}	T_R (min.)	N	D_L/L	T_L/L
JONSWAP	1.0	3.3	6, 8.5	0, -15	10, 20, ∞	20	1440	1.49	1.82
JONSWAP	1.4	3.3	6, 8.5	0, -15	10, 20, ∞	20	1028	0.95	1.16

Test series

Table 2 indicates the characteristics of the waves adopted in the experiments. The spectra were the JONSWAP type with two different peak periods (Tp=1.0s and Tp=1.4s). The peak enhancement factor γ was chosen to be equal to 3.3. The multidirectional waves were simulated by using the well known Single Summation Method in order to eliminate spatial variability of sea states. For the directional spreading function, the Mitsuyasu-type (1975) was chosen, the spreading parameter s was given by the following form (Goda 1985):

$$s = \begin{matrix} S_{max} \cdot \left(f / f_p \right)^5 & : f \leq f_p \\ S_{max} \cdot \left(f / f_p \right)^{-2.5} & : f \geq f_p \end{matrix}$$

Here f_p denotes the frequency at the spectral peak. Values of S_{max} =10, 20 and $S_{max} = \infty$ were applied to simulate multi and unidirectional waves respectively. In order to assess the influence of obliqueness, two different mean angles of incidence $\alpha = 0°$ and $\alpha = -15°$ were used, ensuring at the same time homogeneity of the sea state at the head sections.

In order to minimize statistical variability associated with short lengths of wave records, a recycling period of 20 minutes in model scale was used in the synthesis. This storm duration corresponded to about 1400 waves when Tp=1.0s and 1000 for Tp=1.4s. The ratios of diameter of the head over wave length and length of trunk over wave length are indicated in Table 2.

Table 3 Significant wave heights in the experiments.

Wave Condition	H_{m0}	H_{s_no} (T_p=1.0s)	H_{s_no} (T_p=1.4s)	H_{m0}	H_{s_no} (T_p=1.0s)	H_{s_no} (T_p=1.4s)
Uni Normal ($S_{max}=\infty$)	6.0	6.01	6.17	8.5	8.68	8.42
Uni Oblique ($S_{max}=\infty$)	6.0	6.12	6.15	8.5	8.65	8.66
Multi Normal ($S_{max}=20$)	6.0	5.99	5.99	8.5	8.75	8.70
Multi Oblique ($S_{max}=20$)	6.0	6.16	6.16	8.5	8.77	8.49
Multi Normal ($S_{max}=10$)	6.0	6.01	6.05	8.5	8.63	8.40
Multi Oblique ($S_{max}=10$)	6.0	6.13	5.94	8.5	8.70	8.52

(Units : cm)

Twenty-four test series were carried out using different combinations of spreading index and mean angle of incidence. In each series, the spectrum-based

significant wave heights, H_{mo}, were 6cm and 8.5cm. These sea states were pre-calibrated in the basin without the structure in position, while keeping all wave gauges and current meters in place. The water depth was 30cm.

Table 3 provides a summary of wave heights measured under different experimental combinations without the breakwater model. The values of H_{s_no} are given by averaging the significant wave heights at every wave gauges. It can be found that there is not so much difference between values of H_{mo} and H_{s_no} of incident waves under uni and multidirectional waves.

Characteristics of Velocity Field over Breakwater Head

Armour stones of the breakwaters may be strongly prone to move under a condition of faster flow velocities. Therefore in this study, larger magnitudes of velocities in the time series data of the measurements were discussed. Figure 4 shows the comparison of the U and V component velocities at 4 different locations (CM-2, CM-3, CM-4, CM-5 shown in Figure 1) on the head under 3D waves and those under 2D waves, when H_{mo} is 6cm and Tp is 1.4s. The velocities employed in this figure are the average of the highest 1/3 of the time series data from each current meter. The ordinate in this figure indicates the ratio of the values of U, V for 3D waves to those under 2D waves. Therefore, when these values exceed one, velocities under 3D waves become larger than those under 2D waves. It can be seen that for 3D waves, the V(-) component which is towards the armour layer causing severe damage is larger than those for 2D waves. In even back head section, this value under 3D waves is nearly 1.2 to 1.3 times larger than the values measured under 2D waves.
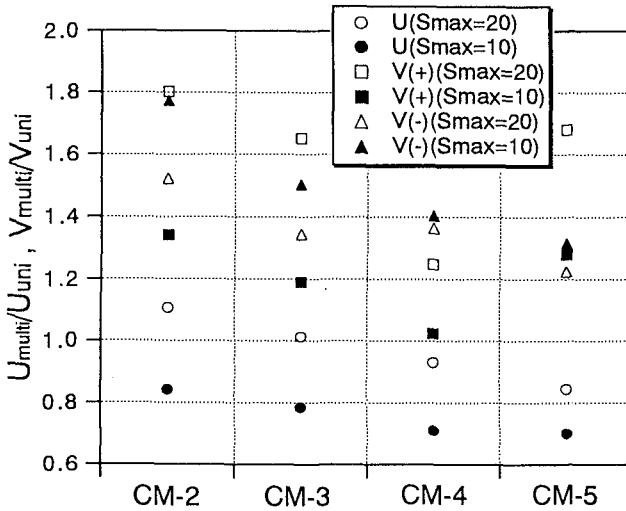

Figure 4 Comparison between U, V component velocities under 3D and 2D waves.

Figure 5 shows the spatial characteristics in correlation of the magnitude of velocity vectors at every current meter. In these figures, the value of R indicates the coefficient of the correlation between measurements at every current meter and that at CM-1 current meter placed on the top of the front head section. It can be seen that in the case of multidirectional waves, the correlation in the middle and back head section is very poor regardless of the mean direction of waves and peak periods. From these results, the possibility of waves attacking directly the heads due to the directional spread associated with 3D waves may be supported.
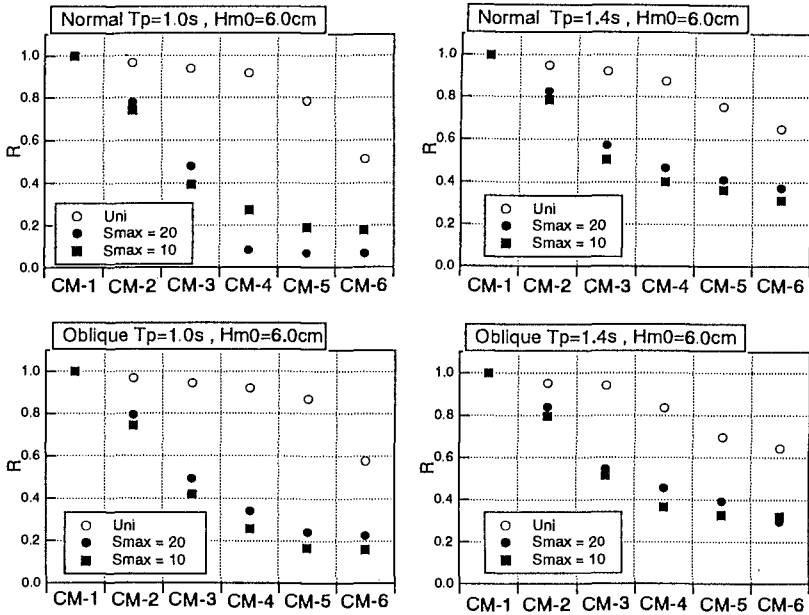

Figure 5 Spatial characteristics in correlation of velocities over the head.

In order to achieve a better understanding of these results, the directionality of velocity vectors on the heads was investigated. Figure 6 (a) and (b) show examples of the directionality of the highest 1/100 of the velocity vectors evaluated from the time series data of U and V at CM-3 (Middle section) and CM-5 (Back section) under 2D and 3D waves, respectively. Especially in the back head section, velocity vectors ($\theta < 0$) under 2D waves wrap around there. Conversely, in the case of 3D waves, the velocity vectors ($\theta > 0$) towards the down-slop of the head appear to be remarkable. The reason may be explained by the influence of the reflection of oblique waves directly attacking the front and middle head sections due to the directional spread in multidirectional waves. From these measurements, it is pointed out that in stability design for the heads, waves attacking directly the front and middle heads in 3D seas cannot be negligible.
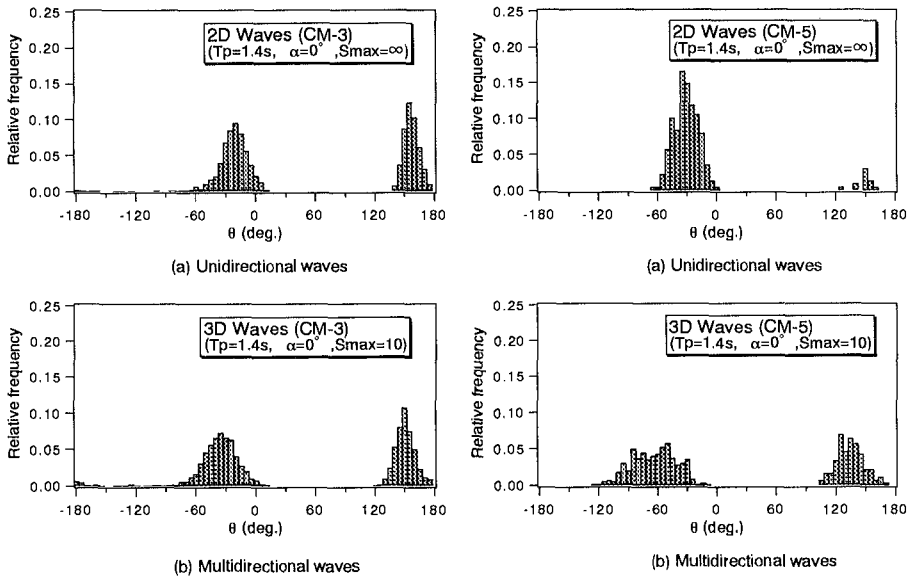
Figure 6 Directionality of velocities over the head.

Consideration on Stability of Armour Stones

The stability of armour stones on the heads is deeply concerned with the magnitudes and directions of the attacking velocity vectors, besides the slope of armour layer with respect to the velocity vectors (Jensen 1984). In this section, an equation about critical current velocity, when the armour stone movement in the heads is brought, is derived by taking account of tangential slope of the heads with respect to the direction of velocity vectors. The sensitive zones of initial damage in the heads will be evaluated by linking this stability formula for armour stones with the measurements of velocity components.

Critical velocity for stability of armour stones

The armour sphere (A) is placed on the head with the horizontal angle β for the velocity vector v_r with horizontal angle θ, as shown in Figure 7. By assuming the shape of the head as a circular cone, the curve of intersection between the vertical plane and the cone becomes a hyperbola. In this study, the only drag force was considered as hydrodynamic force. Then, the equilibrium equation between the armour weight and the drag force can be derived by balancing the moment about point O in this figure:
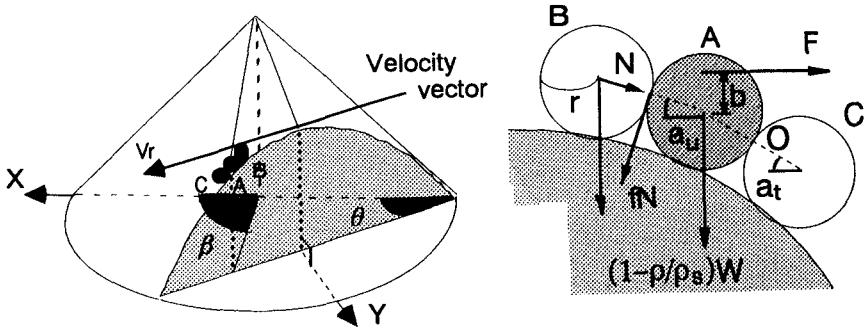
Figure 7   Attacking velocity and hydrodynamics force on armour stone.

$$\left(1 - \frac{\rho}{\rho_s}\right)W\left[\cos a_t + f \sin a_u \left\{1 + \cos\left(a_t - a_u\right)\right\}\right] = F\left(\sin a_t + \frac{b}{r}\right) \qquad (1)$$

where W and r are weight and diameter of armour stone, ρ_s and ρ are unit weight of stone and water, F is drag force, f is friction coefficient between stones. The parameters a_u and a_t in Eq.(1) are respectively the angle of elevation of armour sphere (A) from (C), and (B) from (A) as shown in Figure 7. The drag force is described by the following formula:

$$F = m' \rho \pi r^2 v_r^2 \qquad (2)$$

where m' is drag coefficient of armour stone, v_r is magnitude of attacking velocity vector. The velocity can be expressed by substituting Eq.(2) into Eq.(1) as:

$$\frac{v_r^2}{gr} = \frac{\left(1 - \frac{\rho}{\rho_s}\right)\left[\cos a_t + f \sin a_u \left\{1 + \cos\left(a_t - a_u\right)\right\}\right]}{\frac{3}{4}m'\frac{\rho}{\rho_s}\left(\sin a_t + \frac{b}{r}\right)} \qquad (3)$$

where g is gravitational acceleration. In Eq.(3), f, m', r and b are unknown parameters, a_u and a_t can be derived from tangential slope of the head with respect to the velocity vector as the following.

The cone is mathematically expressed by following formula in X-Y coordinate system shown in Figure 7:

$$Z = a - \frac{1}{2}\sqrt{X^2 + Y^2} \qquad (4)$$

where a is the height of the cone, Z is distance from bottom. The coordinate (X,Y) of center of armour sphere (A) becomes $\left(R\cos(\beta-\theta), R\sin(\beta-\theta) \right)$ in X-Y coordinate system. The tangential slope of the heads with respect to the velocity vector can be derived by partially differentiating Eq.(4) with respect to X, and inserting the (X,Y) of the point A:

$$\text{Tangential slope} = -\frac{1}{2}\cos(\beta-\theta) \tag{5}$$

Assuming that a_t is equal to a_u for simplicity in this study, they are given as:

$$a_t = a_u = \tan^{-1}\left\{ \frac{1}{2}\cos(\beta-\theta) \right\} \tag{6}$$

Finally, the critical velocity, v_{rc}, for armour stone movement in the heads is expressed by substituting Eq.(6) for a_t and a_u into Eq.(3):

$$\frac{v_{rc}^2}{gr} = \frac{\left(1 - \frac{\rho}{\rho_s}\right)\left\{1 + f\cos(\beta-\theta)\right\}}{\frac{3}{4}m'\left(\frac{\rho}{\rho_s}\right)\left[\frac{\cos(\beta-\theta)}{2} + \frac{b}{r}\sqrt{1 + \left\{\frac{\cos(\beta-\theta)}{2}\right\}^2} \right]} \tag{7}$$

When the tangential slope with respect to attacking velocity vector becomes positive, in Eq.(7), the plus sign before the friction coefficient, f, is replaced by the minus sign. The unknown parameters m', b and f in Eq.(7) were considered as $m'=1$, $b=0.5r$ and $f=0.4$, for simplicity in this paper.
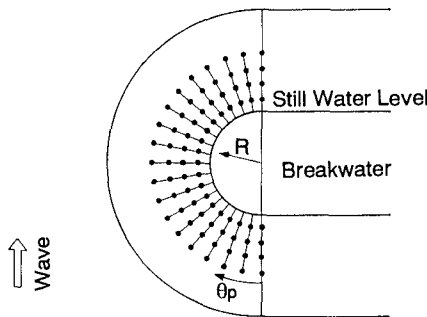

Figure 8 Measuring points of velocity components over the head.

Influence of wave directionality on sensitive zone for initial damage

        In this section, in order to investigate the influence of wave directionality on
the stability of breakwater heads, the spatial occurrence frequencies for armour
stone movement in the head sections were estimated by linking Eq.(7) and the
velocity vectors which were newly measured at 76 points over the head shown in
Figure 8.
        Figure 9(a) and 9(b) show the spatial distribution of calculated occurrence
frequencies for armour stone movement in the head under conditions of the normal
3D waves and 2D waves with Tp=1.4s and H_{m0}=6cm respectively, in which θp is
the angle from the front head and R is the distance in the radial direction from the
center of head as shown in Figure 8. In these figures, contour lines of relative
occurrence frequencies which are normalized with respect to the total number of
velocities measured for 20 minutes are indicated with interval every 0.002.
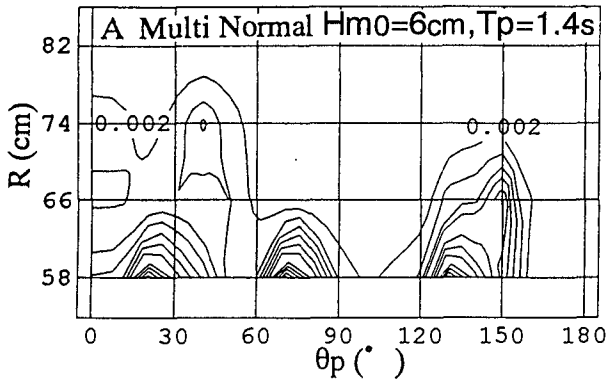
(a) Multidirectional waves (S_{max} = 10)
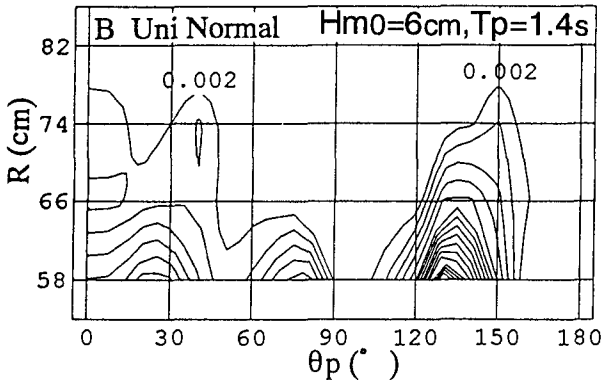
(b) Unidirectional waves (S_{max} = ∞)

Figure 9 Spatial distribution of occurrence frequencies for armour stone movement.

In order to investigate the reliability of those calculated results, the initial damage tests of armour stones in the head sections were carried out under the same incident wave conditions as those in the velocity measuring tests. The resulting initial damage zones in the head under 3D and 2D waves attack are shown in Figure 10(a) and 10(b), respectively. In these figures, the hatched parts mean that the second armour layer is clearly exposed due to the displacement of the first armour layer. By comparing these initial damage patterns with the spatial distributions of occurrence frequencies for armour stone movement shown in Figure 9, it can be seen that the results of the calculations evaluating the locations of the initial damage are fairly close to the experimental locations.

Hm=6cm,Tp=1.4s   Hm=6cm,Tp=1.4s

(a) Multidirectional waves
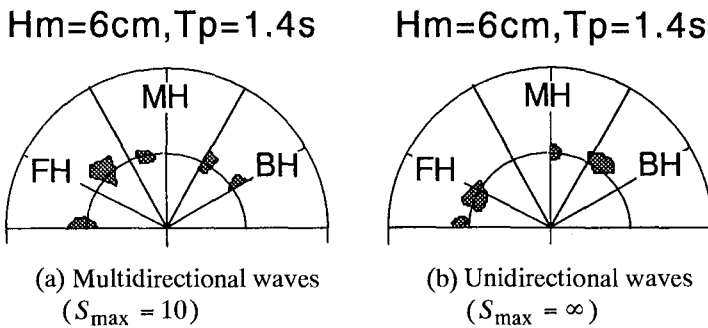$(S_{max} = 10)$

(b) Unidirectional waves
$(S_{max} = \infty)$

Figure 10 Initial damage zones in the head.

It can be found from Figure 9 that the sensitive zones for armour stone movement in the head sections are appeared at three locations; the front, middle and back head section respectively. Although there is not so much difference in these locations under 3D and 2D waves, there is obvious difference between the values of both occurrence frequencies, that is, in the case of the unidirectional waves, the back head section is more sensitive part for armour stone movement. Under unidirectional waves attack, it could be observed in the damage tests that the damage in the back head section was caused to plunge of the strong current with the high velocities generated by refraction, shoaling and diffraction processes. On the other hand, under multidirectional waves attack, the front and middle section are more sensitive part for the initial damage, because of the oblique waves attacking directly these sections due to the directional spread associated with the multidirectional seas. This consideration may be supported, since in the case of the multidirectional waves of Figure 6(b), the direction (θ>0) of velocity vectors outwards from the armour layer in the back head section is remarkably recognized in comparison with those under unidirectional waves.

Under oblique incidence, the multidirectional waves resulted in larger occurrence frequencies in the three sensitive zones (FH, MH and BH) for armour

stone movement than those under unidirectional waves. This is caused by the waves attacking directly the back head section due to the oblique incidence. When Tp was equal to 1.0s, the difference in calculated occurrence frequencies for armour movement in the head sections between uni and multidirectional waves was relatively small.

Conclusion

In this study, the characteristics of velocity field over the head under 2D and 3D waves were investigated. The V velocity component under multidirectional waves was larger than those under unidirectional waves. A noteworthy finding was that those on the back head section under 3D waves were larger by nearly 1.2 to 1.3 times the values measured under 2D waves, and that the direction of velocity vectors downing slop in the back section under 3D waves were remarkably recognized.

The presented equation of the critical velocity for armour stone movement in the heads could satisfactorily explain the initial damage zones in the damage tests. The front and middle head section were more sensitive zone for the initial damage under multidirectional waves attack. This result provided a better insight into previous study.

Further the unknown parameter in the presented equation will be investigated by physical experiments or theoretical techniques, the stability of breakwater heads will be evaluated by linking the equation of the critical velocity for armour stone movement with a numerical analysis of wave kinematics over the heads.

References

Jensen, O.J. (1984). "A monograph on rubble mound breakwaters", Danish Hydraulics Institute, Denmark.

Matsumi, Y., Mansard, E.P.D. and Rutledge, J. (1994). "Influence of wave directionality on stability of breakwater heads", Proc. 26th Int. Conf. on Coast. Engrg., ASCE, 1397-1411.

Mitsuyasu, H. et al (1975). "Observation of the directional spectrum of ocean waves using a cloverleaf buoy", Jour. Physical Oceanography, Vol.5, 750-760.

Van der Meer, J.W. (1987). "Stability of breakwater armour layers - design formulae", Coastal Engrg., 219-239.

Y. Goda (1985). Random seas and design of maritime structures, University of Tokyo Press, Japan.